# Electronic Supplementary Information

## Ru nanodendrites composed of ultrathin fcc/hcp nanoblades for hydrogen evolution reaction in alkaline solution

Kai Gao,[a] Yao Wang,[a,b] Zhiwei Wang,[a] Zhaohua Zhu,[a] Jialiang Wang,[a] Zhimin Luo,[b] Cong Zhang,*[a] Xiao Huang,*[a] Hua Zhang,*[b] and Wei Huang[a,c]

[a]Key Laboratory of Flexible Electronics (KLOFE) & Institute of Advanced Materials (IAM), Nanjing Tech University (NanjingTech), 30 South Puzhu Road, Nanjing 211816, P.R. China
[b]Center for Programmable Materials, School of Materials Science and Engineering, Nanyang Technological University, 50 Nanyang Avenue, Singapore 639798, Singapore
[c]Shaanxi Institute of Flexible Electronics (SIFE), Northwestern Polytechnical University (NPU), 127 West Youyi Road, Xi'an 710072, China

### 1. Experimental Section

### 1.1 Chemicals and materials

Ruthenium (Ⅲ) acetylacetonate (Ru(acac)$_3$, 97%), copper (II) chloride dehydrate ($CuCl_2 \cdot 2H_2O$, 99%), benzyl alcohol (99-100.5%), copper (II) sulfate pentahydrate ($CuSO_4 \cdot 5H_2O$, 98%) and nafion perfluorinated resin solution (5 wt.%) were purchased from Sigma-Aldrich (Beijing, China). Platinum on carbon (20 wt.%) was purchased from Shanghai Hesen Electric Co., Ltd (Shanghai, China). Ascorbic acid ($C_6H_8O_6$, AA), polyvinylpyrrolidone (PVP, K30), ammonium hydroxide ($NH_3 \cdot H_2O$, AR), hydrochloric acid (HCl, AR), nitric acid ($HNO_3$, AR), hydrogen peroxide solution ($H_2O_2$, AR), sulfuric acid ($H_2SO_4$, 98%) and carbon black (CB) were purchased from Sinopharm Chemical Reagent Co. Ltd. (Shanghai, China). Potassium hydroxide (KOH, 85%) was purchased from J&K Chemical (Shanghai, China). The deionized water was obtained from the Milli-Q3 System (Millipore, France). All the materials were used as received without further purification.

### 1.2 Synthesis of RuCu NDs and Ru NDs

8 mg of Ru(acac)$_3$, 3.5mg of $CuCl_2 \cdot 2H_2O$, 50 mg of AA and 100 mg of PVP were dissolved in 12 mL benzyl alcohol and heated at 90 °C under stirring for 30 min. The resultant homogeneous pink solution was then transferred into a 25 mL Teflon-lined

stainless steel autoclave and then heated at 160 °C for 10 h. After being cooled down to room temperature, the resulting RuCu NDs were collected by centrifugation at 10000 rpm for 10 min, washed three times with acetone/ethanol (1:1 in volume), and then re-dispersed in ethanol for further characterizations.

The aforementioned RuCu NDs were collected by centrifugation and re-dispersed in a mixture containing 0.5 mL $H_2O_2$, 2 mL $NH_3{\cdot}H_2O$ and 10 mL $H_2O$. This mixture was then stirred at room temperature for 48 h to selectively remove Cu in the dendritic nanostructures via the following reaction: $Cu + H_2O_2 + 4NH_3{\cdot}H_2O = [Cu(NH_3)_4](OH)_2 + 4H_2O$.[1] The resulting Ru NDs were collected by centrifugation at 10000 rpm for 10 min, washed three times with deionized water and three times with ethanol in turn, and finally re-dispersed in ethanol for further characterizations.

## 1.3 Characterizations

The crystal structures of the products were studied by powder X-ray diffraction (XRD) on a Smartlab Rigaku diffractometer equipped with Cu Kα radiation ($\lambda$ = 1.54 Å). The morphologies, microstructures and elemental distribution of the products were investigated by transmission electron microscopy (TEM, JEOL 2100, Japan) and high resolution transmission electron microscope (HRTEM, JEOL 2100F, Japan) coupled with energy dispersive X-ray (EDX) spectroscope. X-ray photoelectron spectroscopy (XPS, PHI 5000 Versa Probe, Japan) measurements were conducted on the metal nanostructures, and the binding energies were corrected for specimen charging effects using the C 1s level at 284.6 eV as the reference. Brunauer-Emmett-Teller (BET, Micromeritics, ASAP2460, USA) measurements were used to measure the specific surface area and pore size distribution of various samples. Inductively coupled plasma optical emission spectrometry (ICP-OES, PE5300DV, USA) was used to measure the ion concentrations of solutions containing dissolved metal nanostructures.

## 1.4 Electrochemical measurements

To ensure a good dispersion of metal catalysts on commercial carbon black, hydrophilic treatment of the carbon black was carried out based on a previous report.[2] Typically, 0.6 g of commercial carbon black was added into 10 mL HCl (20%) in a 25 mL Teflon-lined stainless steel autoclave and then heated at 120 °C for 10 h. After being cooled down to room temperature, the resulting product was collected by centrifugation at 10000 rpm for 10 min and then transferred to a 25 mL Teflon-lined stainless steel autoclave together with 10 mL $HNO_3$ (5.0 M). After being heated at 120 °C for 10 h, the product was collected by filtration and washing, followed by drying in an oven at 150 °C for 8 h.

The concentration of Ru in Ru NDs or RuCu NDs solution was measured by ICP-OES. Based on this concentration, we calculated the volume of Ru NDs or RuCu NDs solution needed to give 2 mg Ru. After that the solution containing 2 mg Ru was centrifuged at high speed (10000 rpm for 15 min) and re-dispersed in 2 mL of a mixture containing water, ethanol and nafion (5%) with a volumetric ratio of $V_{water}$: $V_{ethanol}$: $V_{nafion} = 1:1:0.04$, followed by the addition of 8 mg acid treated-carbon black to form a homogeneous catalyst dispersion by sonication for 30 min.

The electrochemical HER measurements were carried out in a three-electrode system on an electrochemical station (Autolab PGSTAT 302N) coupled with a rotating disk electrode (RDE). A standard Ag/AgCl electrode was used as the reference electrode and a graphite rod was used as the counter electrode. A glassy carbon (GC) disk electrode (3.0 mm in diameter) was firstly polished with alumina slurries ($Al_2O_3$, 0.05 μm) on a polishing cloth to obtain a mirror finish. Then 2.5 μL of the aforementioned catalyst dispersion was drop-casted on the polished electrode surface and allowed to dry naturally, and thus the loading of the active material (i.e. Ru) on GC was calculated to be 35.4 $\mu g/cm^2$. All potentials reported in this work were calibrated and converted to the reversible hydrogen electrode (RHE). Polarization curves were acquired in 1 M KOH electrolyte over a potential range of -0.4 to -0.1 V vs. RHE with a scan rate of 2 mV $s^{-1}$ and a rotation speed of 1600 rpm. Electrochemical impedance spectroscopy (EIS) analysis was carried out with an amplitude of 5 mV over a frequency range of 100 kHz to 0.1 Hz in 1 M KOH. Before the tests, the electrolyte was purged with $N_2$ for 30 min. The accelerated durability tests (ADTs) were conducted in 1 M KOH by applying the cyclic potential sweeps at a sweep rate of 100 mV/s for 1000 cycles. Chronoamperometry analysis was performed under a constant potential of -0.05 V vs. RHE in 1 M KOH solution.

### 1.5 Calculation of electrochemical active surface area (ECSA)

Electrochemical capacitances were measured by cyclic voltammograms (CV) in 1 M KOH at different scan rates of 20, 40, 60, 80, 100, 120, 140, 160, 180, and 200 mV $s^{-1}$ for Ru ND/C, RuCu ND/C, and Ru ND/C synthesized without presence of $Cu^{2+}$ as shown in Fig. S8. The capacitive currents were collected where no apparent Faradic processes were observed. These measured capacitive currents were then plotted as a function of scan rate in Fig. 3c. Linear fitting of the plots revealed that the specific capacitances were 22.2, 18.1 and 7.6 mF $cm^{-2}$ for Ru ND/C, RuCu ND/C and Ru ND/C synthesized without presence of $Cu^{2+}$ respectively. The specific capacitance for a flat surface is generally found to be in the range of 20~60 μF $cm^{-2}$. Therefore, by assuming the specific capacitance as ~40 μF $cm^{-2}$ for 1 $cm^2$ of active catalyst surface area, the ECSA is estimated as follows:[3-5]

$$A_{ECSA}^{Sample} = \frac{specfic\ \ capacitance}{40\ \ \mu\text{F}\ \ cm^{-2}\ \text{per}\ \ cm_{ECSA}^{2}}$$

For example, the ECSA of Ru ND/C in 1 M KOH was calculated as:

$$A_{ECSA}^{Ru\ ND/C} = \frac{22.2\ \ \mu\text{F}\ \ cm^{-2}}{40\ \ \mu\text{F}\ \ cm^{-2}\ \text{per}\ \ cm_{ECSA}^{2}} = 555\ \ cm_{ECSA}^{2}$$

The ECSA values of RuCu ND/C and Ru ND/C synthesized without presence of $Cu^{2+}$ were 453 and 190 $cm^2$, respectively.

## II. Supplementary Figures and Tables

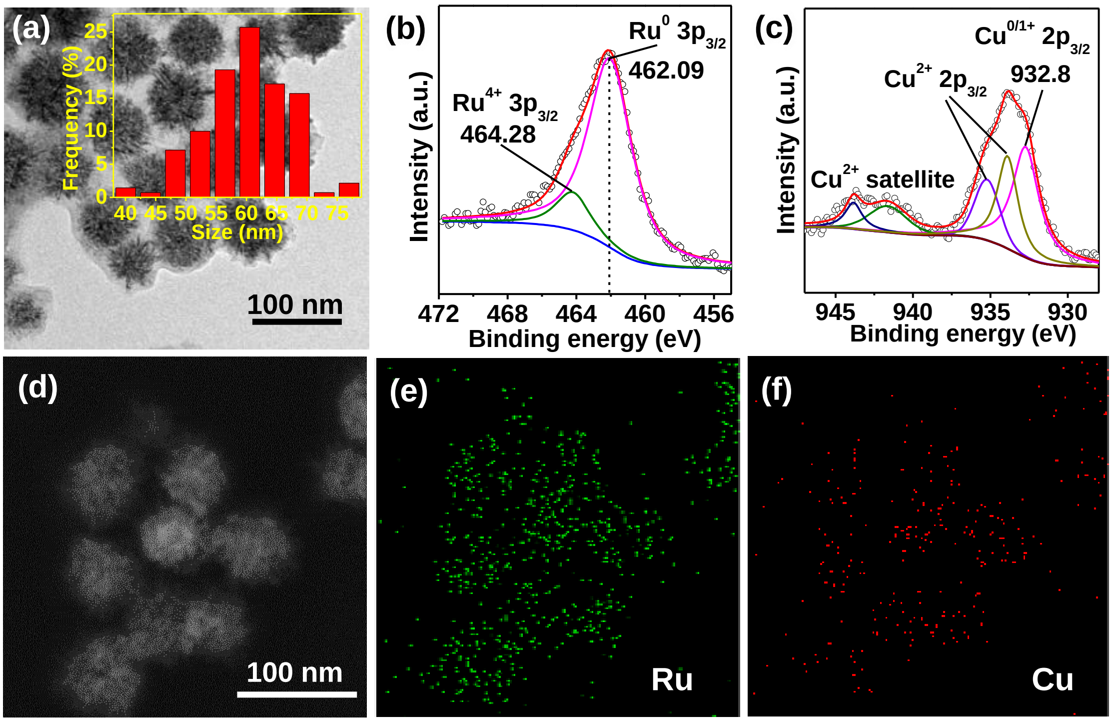

**Fig. S1** (a) TEM image of RuCu NDs. Inset: size distribution of the RuCu NDs. XPS (b) Ru 3p and (c) Cu 2P spectra of RuCu NDs. (d) STEM image and the corresponding EDX mapping of RuCu NDs showing presence of (e) Ru and (f) Cu, respectively.

From the XPS spectrum in Fig. S1b, it is noted that the peak centered at 462.09 eV can be assigned to Ru (0) $3p_{3/2}$, which further confirms the dominating metallic state of Ru in NDs (Fig. S1b, ESI) despite the fact that slight Ru (IV) in the oxidation state (464.28 eV) was present with an estimated concentration of 13.62%.[6,7] Fig. S1c shows the Cu $2p_{3/2}$ spectrum, where the binding energy at 932.8 eV suggests the presence of Cu (I) or Cu (0), and the binding energies at 935.3 eV, 933.9 eV and 941.7-943.8 eV were assigned to Cu (II), indicating the partial oxidation of Cu.[8-10]

**Table S1.** Concentrations of Cu and Ru in RuCu NDs and Ru NDs based on ICP-OES measurements.

| Product | Element | Atomic percentage |
|---|---|---|
| RuCu NDs | Cu | 45% |
|  | Ru | 55% |
| Ru NDs | Cu | 8% |
|  | Ru | 92% |

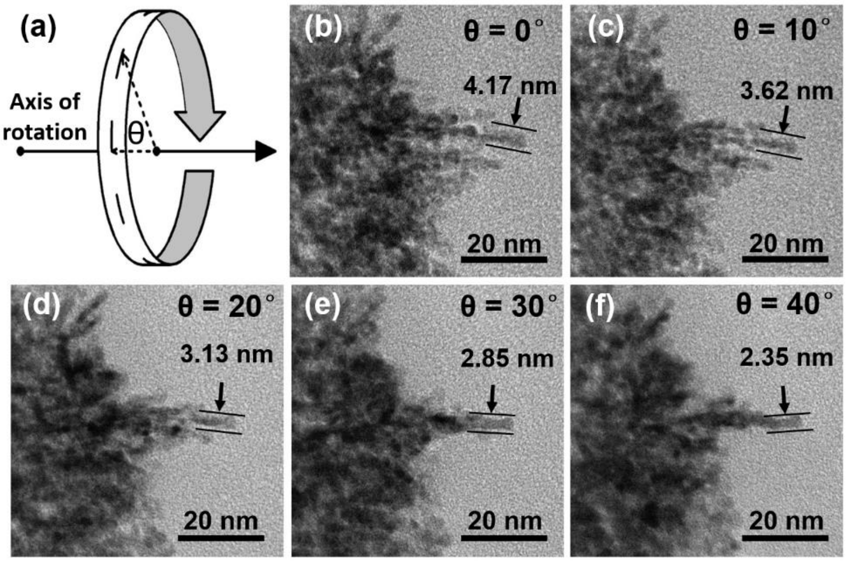

**Fig. S2** (a) Schematic drawing of the tilting experiment. A series of TEM images showing a particular nanoblade on a Ru ND as the sample holder was tilted at different angles: (b) 0°, (c) 10°, (d) 20°, (e) 30°, and (f) 40°.

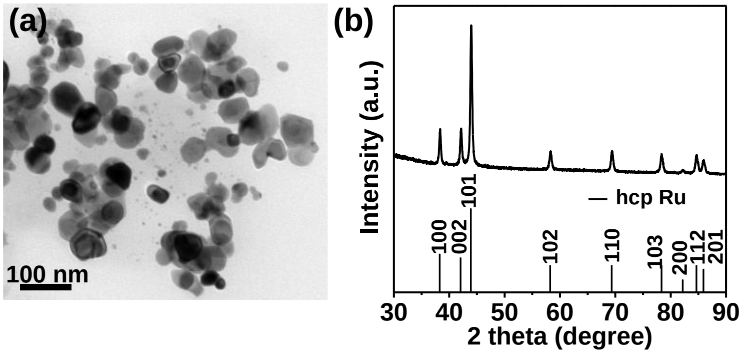

**Fig. S3** (a) TEM image and (b) XRD pattern of Ru NDs after being heated at 700 ℃.

**Table S2.** Atomic ratios of Cu : Ru in RuCu NDs obtained at different reaction intervals based on EDX analysis.

| **Reaction time (h)** | **1** | **2** | **4** |
|---|---|---|---|
| **Cu : Ru (atomic ratio)** | **1 : 3.4** | **1 : 2.4** | **1 : 1.6** |

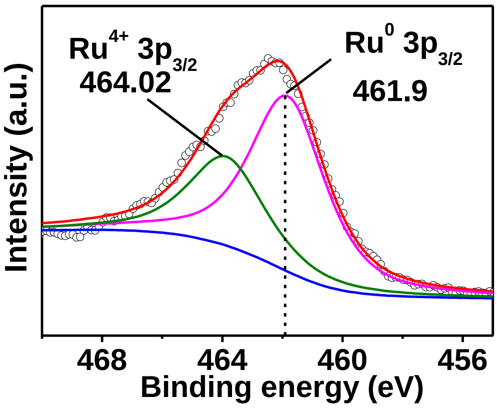

**Fig. S4** XPS Ru 3p spectrum of Ru NDs.

The peak centered at 461.9 eV corresponds to Ru (0) 3p$_{3/2}$, and that at 464.02 eV corresponds to Ru (IV).[6,7] The concentration of the Ru (IV) shoulder, as compared with that in Fig. S1b, increased from 13.62% to 34.14%.

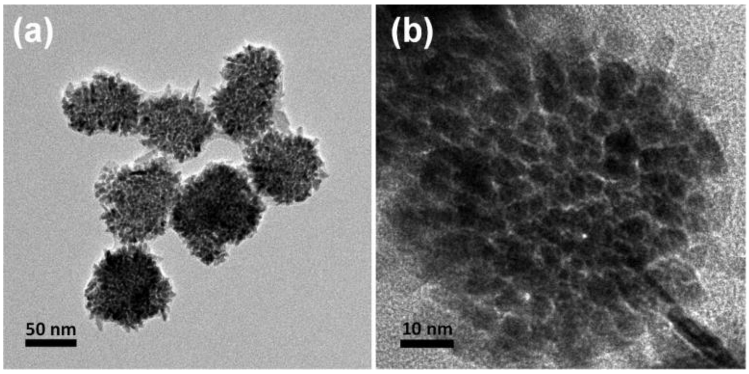

**Fig. S5** (a,b) TEM images of Ru NDs synthesized without presence of Cu$^{2+}$ precursor.

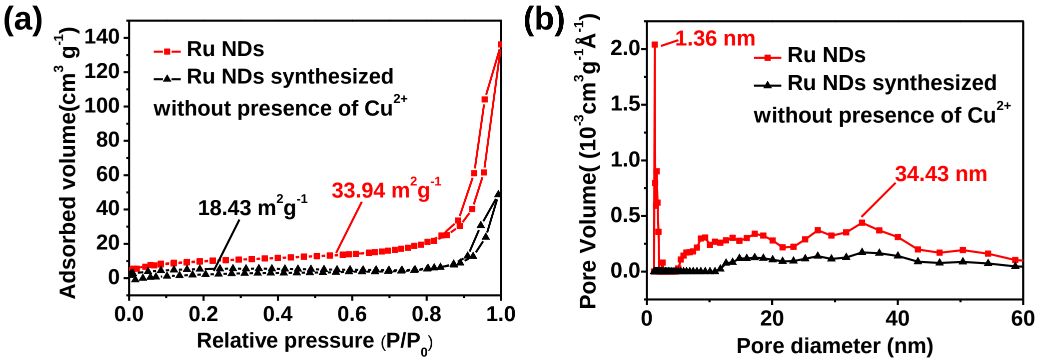

**Fig. S6** (a) $N_2$ adsorption/desorption isotherms and (b) pore size distribution of Ru NDs and Ru NDs synthesized without presence of $Cu^{2+}$ precursor.

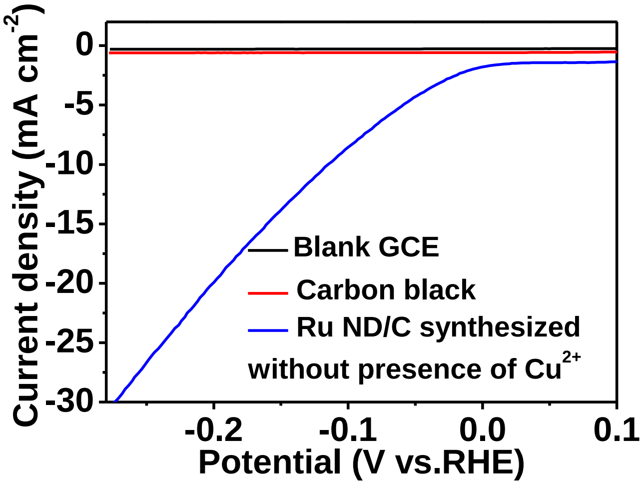

**Fig. S7** Linear sweep voltammetry (LSV) curves of blank GC electrode (GCE), carbon black, and Ru NDs synthesized without presence of $Cu^{2+}$.

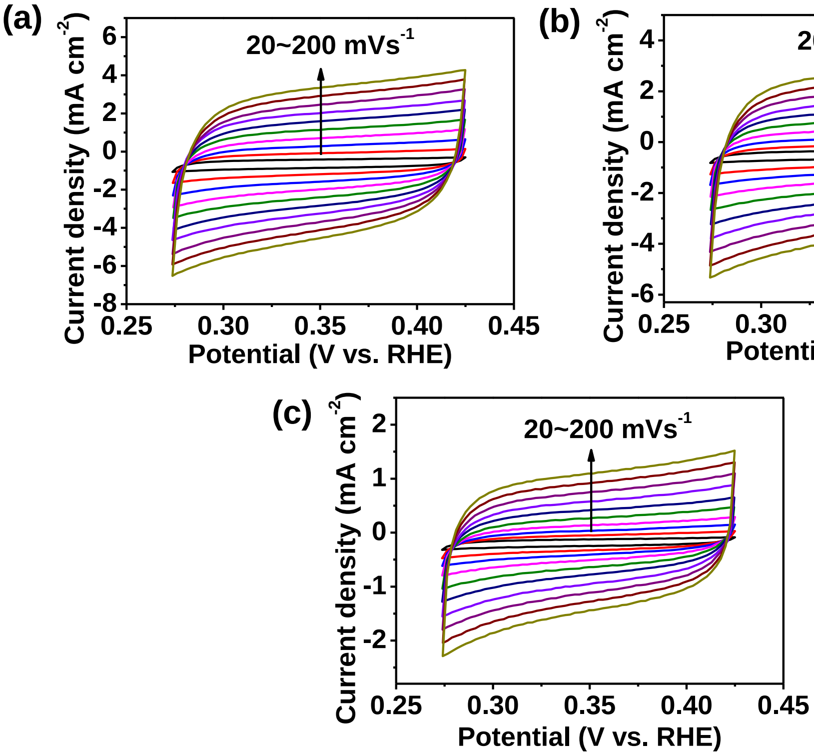

**Fig. S8** CV curves in 1 M KOH for (a) Ru ND/C, (b) RuCu ND/C and (c) Ru ND/C synthesized without presence of Cu$^{2+}$ in a potential range of 0.27~0.42 V vs. RHE. The capacitive currents were collected at 0.35 V vs. RHE where no Faradaic processes were present.

Electrochemical capacitances were measured by cyclic voltammograms (CV) in 1 M KOH at different scan rates of 20, 40, 60, 80, 100, 120, 140, 160, 180, and 200 mV s$^{-1}$ for Ru ND/C, RuCu ND/C, and Ru ND/C synthesized without presence of Cu$^{2+}$ as shown in Fig. S8. The capacitive currents were collected where no apparent Faradic processes were observed. These measured capacitive currents were then plotted as a function of scan rate in Fig. 3c. Linear fitting of the plots revealed that the specific capacitances were 22.2, 18.1 and 7.6 mF cm$^{-2}$ for Ru ND/C, RuCu ND/C and Ru ND/C synthesized without presence of Cu$^{2+}$ respectively. The specific capacitance for a flat surface is generally found to be in the range of 20~60 μF cm$^{-2}$. Therefore, by assuming the specific capacitance as ~40 μF cm$^{-2}$ for 1 cm$^2$ of active catalyst surface area, the ECSA is estimated as follows:[3-5]

$$A_{ECSA}^{Sample} = \frac{specfic\ \ capacitance}{40\ \ \mu\text{F}\ \ cm^{-2}\ \ \text{per}\ \ cm_{ECSA}^{2}}$$

For example, the ECSA of Ru ND/C in 1 M KOH was calculated as:

$$A_{ECSA}^{Ru\ \ ND/C} = \frac{22.2\ \ \mu\text{F}\ \ cm^{-2}}{40\ \ \mu\text{F}\ \ cm^{-2}\ \ \text{per}\ \ cm_{ECSA}^{2}} = 555\ \ cm_{ECSA}^{2}$$

The ECSA values of RuCu ND/C and Ru ND/C synthesized without presence of $Cu^{2+}$ were 453 and 190 $cm^2$, respectively.

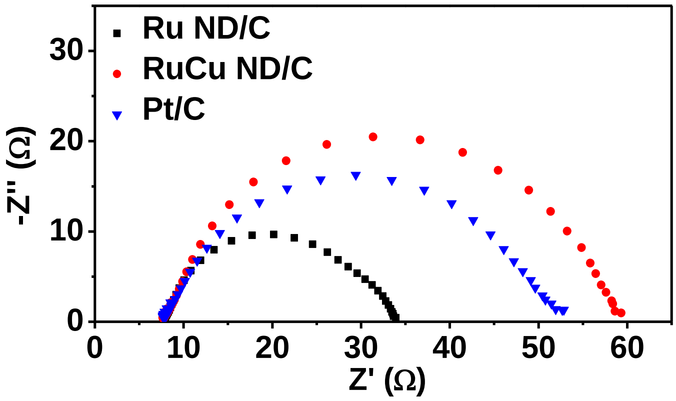

**Fig. S9** Nyquist plots measured for Ru ND/C, RuCu ND/C and Pt/C in 1 M KOH over the frequency range of 100 kHz to 0.1 Hz in 1 M KOH. It can be seen that the Nyquist plots are nearly semicircles. In general, the diameters of the semicircles are associated with the charge transfer resistance ($R_{CT}$) at the interface between the electrode and the electrolyte. The $R_{CT}$ of Ru ND/C is estimated to be 26.17 Ω, which is smaller than that of Pt/C (44.93 Ω) and RuCu ND/C (50.88 Ω) in 1 M KOH.

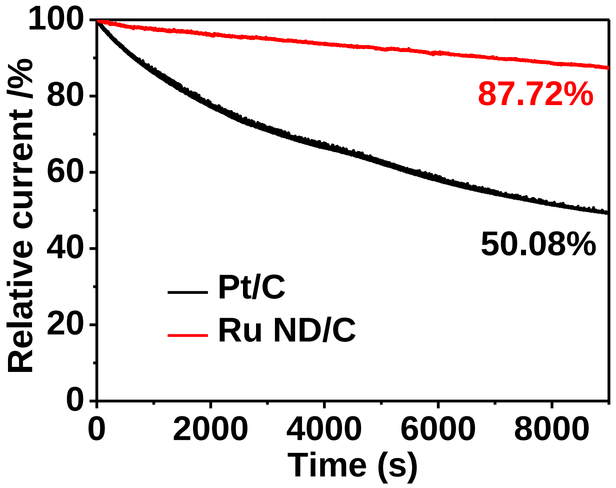

**Fig. S10** Normalized current-time (i–t) chronoamperometric responses for HER at Ru ND/C and commercial Pt/C electrodes under a constant potential of -0.05 V vs RHE in 1 M KOH solution.

**Table S3.** Summary of recently reported state-of-the-art HER electrocatalysts in alkaline electrolytes.

| Catalyst | Loading amount (µg cm$^{-2}$) | Electrolyte (KOH) | Overpotential at 10 mA cm$^{-2}$ (mV) | Tafel slope (mV dec$^{-1}$) | Reference |
|---|---|---|---|---|---|
| Ru ND/C | 35.4 (Ru);<br>176.8 (Total) | 1 M | 43.4 | 49 | This work |
| $Pt_3Ni/NiS/C$ | 15.3 (Pt) | 0.1 M<br>1 M | > 100<br>< 60 | | Nat. Commun., 2017[11] |
| $Pd/FeO_x(OH)_{2-2x}/C$ | 127 (total) | 0.1 M | | 131 | Adv. Energy Mater., 2017[12] |
| $Pt_3Ni_3$ nanowires/C | 15.3 (Pt) | 1 M | 40 | | Angew. Chem. Int. Ed., 2016[13] |
| Pt NWs/SL-$Ni(OH)_2$ | 6.12 (Pt) | 0.1 M | <100 | | Nat. Commun., 2015[14] |
| Pt–Ni alloy nanomultipods/C | 7.65 (Pt)<br>61.22 (total) | 0.1 M | 65 | 78 | Nat. Commun., 2017[15] |
| Pt–Ni/C and Pt–Ni/C-HAc | 4.2(Pt) | 0.1 M | ~75 | ~60 | J. Mater. Chem. A, 2016[16] |
| $Co_2P$ (O- $Co_2P$-3) | 200 (total) | 1 M | | 61.1 | Adv. Mater., 2017[17] |

| | | | | | |
|---|---|---|---|---|---|
| NiO/Ni-CNT | 400 (total) | 1 M | ~100 | 82 | Nat. Commun., 2014[18] |
| Cu-Ti | | 0.1 M | ~50 | 110 | Nat. Commun., 2015[19] |
| RuCo@NC | 275 (total) | 1 M | 28 | 31 | Nat. Commun., 2017[20] |
| Ru@$C_2N$ | 285 (total) | 1 M | <50 | 38 | Nat. Nanotechnol., 2017[21] |
| Ru/$C_3N_4$/C | 204 (total) | 0.1 M | 79 | | J. Am. Chem. Soc., 2016[22] |
| NF-$Ni_3Se_2$/Ni | 8870 (total) | 1 M | 203 (with iR-correction) | 79 | Nano Energy, 2016[23] |
| Pd-CNX | 280 (total) | 0.5 M | 180 ($\eta_5$) | 150 | ACS Catal., 2016[24] |
| $Mo_2C$@N-C | 280 (total) | 1 M | 60 | | Angew. Chem. Int. Ed., 2015[25] |
| Ni-Mo-N | $10^3$ (total) | 1 M | 43 ($\eta_{20}$) | 40 | Nano Energy, 2016[26] |
| $MoO_X$/$Ni_3S_2$/NF | $12*10^3$ (total) | 1 M | 110 ($\eta_{15}$) | 90 | Adv. Funct. Mater., 2016[27] |
| $CoO_X$@CN | 420 (total) | 1 M | 232 | | J. Am. Chem. Soc., 2015[28] |
| $CoP_2$/RGO | 285 (total) | 1 M | 88 (with iR-correction) | 50 | J. Mater. Chem. A, 2016[29] |
| CoP/rGO-400 | 280 (total) | 1 M | 150 | 38 | Chem. Sci., 2016[30] |

## REFERENCES

1 K. O. -Asake and K. K. Mishra, *J. Electron. Mater.,* 1996, **25**, 1599.

2 M. Y. Liu, Z. P. Xiang, H. Q. Deng, K. Wan, Q. B. Liu, J. H. Piao, Y. Y. Zheng and Z. X. Liang, *J. Electrochem. Soc.,* 2016, **163**, H1.

3 Y. Y. Chen, Y. Zhang, W. J. Jiang, X. Zhang, Z. Dai, L. J. Wan and J. S. Hu, *ACS Nano*, 2016, **10**, 8851.

4 R. Zhang, X. Wang, S. Yu, T. Wen, X. Zhu, F. Yang, X. Sun, X. Wang and W. Hu, *Adv. Mater.*, 2017, **29**, 1605502.

5 R. Ye, Y. Liu, Z. Peng, T. Wang, A. S. Jalilov, B. I. Yakobson, S. H. Wei and J. M. Tour, *ACS Appl. Mater. Interfaces*, 2017, **9**, 3785.

6 N. Chakroune, G. Viau, Souad Ammar, L. Poul, D. Veautier, M. M. Chehimi, C. Mangeney, F Villain and F Fiévet, *Langmuir,* 2005, **21**, 6788.

7 Z. Zhang, Y. Liu, B. Chen, Y. Gong, L. Gu, Z. Fan, N. Yang, Z. Lai, Y. Chen, J. Wang, Y. Huang,

M. Sindoro, W. Niu, B. Li, Y. Zong, Y. Yang, X. Huang, F. Huo, W. Huang and H. Zhang, *Adv. Mater.*, 2016, **28**, 10282.

8 S. G. Chen, Y. J. Guo, S. J. Chen, H. M. Yu, Z. C Ge, X Zhang, P. X. Zhang and J. N. Tang, *J Mater. Chem.*, 2012, **22**, 9092.

9 P. Liu and E. J. M. Hensen, *J. Am. Chem. Soc.*, 2013, **135**, 14032.

10 F. Coloma, F. Marquez, C. H. Rochesterc and J. A. Anderson, *Phys. Chem. Chem. Phys.*, 2000, **2**, 5320.

11 P. Wang, X. Zhang, J. Zhang, S. Wan, S. Guo, G. Lu, J. Yao and X. Huang, *Nat. Commun.*, 2017, **8**, 14580.

12 H. Liao, C. Wei, J. Wang, A. Fisher, T. Sritharan, Z. Feng and Z. J. Xu, *Adv. Energy Mater.*, 2017, **7**, 1701129.

13 P. Wang, K. Jiang, G. Wang, J. Yao and X. Huang, *Angew. Chem. Int. Ed.*, 2016, **55**, 12859.

14 H. Yin, S. Zhao, K. Zhao, A. Muqsit, H. Tang, L. Chang, H. Zhao, Y. Gao and Z. Tang, *Nat. Commun.*, 2015, **6**, 6430.

15 Z. Cao, Q. Chen, J. Zhang, H. Li, Y. Jiang, S. Shen, G. Fu, B. A. Lu, Z. Xie and L. Zheng, *Nat. Commun.*, 2017, **8**, 15131.

16 R. Kavian, S. -I. Choi, J. Park, T. Liu, H. -C. Peng, N. Lu, J. Wang, M. J. Kim, Y. Xia and S. W. Lee, *J. Mater. Chem. A*, 2016, **4**, 12392-12397.

17 K. Xu, H. Ding, M. Zhang, M. Chen, Z. Hao, L. Zhang, C. Wu and Y. Xie, *Adv. Mater.*, 2017, **29**, 1606980.

18 M. Gong, W. Zhou, M. C. Tsai, J. Zhou, M. Guan, M. C. Lin, B. Zhang, Y. Hu, D. Y. Wang, J. Yang, S. J. Pennycook, B. J. Hwang and H. Dai, *Nat. Commun.*, 2014, **5**, 4695.

19 Q. Lu, G. S. Hutchings, W. Yu, Y. Zhou, R. V. Forest, R. Tao, J. Rosen, B. T. Yonemoto, Z. Cao, H. Zheng, J. Q. Xiao, F. Jiao and J. G. Chen, *Nat. Commun.*, 2015, **6**, 6567.

20 J. Su, Y. Yang, G. Xia, J. Chen, P. Jiang and Q. Chen, *Nat. Commun.*, 2017, **8**, 14969.

21 J. Mahmood, F. Li, S. M. Jung, M. S. Okyay, I. Ahmad, S. J. Kim, N. Park, H. Y. Jeong and J. B. Baek, *Nat. Nanotechnol.*, 2017, **12**, 441.

22 Y. Zheng, Y. Jiao, Y. Zhu, L. H. Li, Y. Han, Y. Chen, M. Jaroniec and S. Z. Qiao, *J. Am. Chem. Soc.*, 2016, **138**, 16174.

23 R. Xu, R. Wu, Y. Shi, J. Zhang and B. Zhang, *Nano Energy*, 2016, **24**, 103.

24 T. Bhowmik, M. K. Kundu and S. Barman, *ACS Catal.*, 2016, **6**, 1929.

25 Y. Liu, G. Yu, G. D. Li, Y. Sun, T. Asefa, W. Chen and X. Zou, *Angew. Chem. Int. Ed.*, 2015, **54**, 10752.

26 T. Wang, X. Wang, Y. Liu, J. Zheng and X. Li, *Nano Energy*, 2016, **22**, 111.

27 Y. Wu, G.-D. Li, Y. Liu, L. Yang, X. Lian, T. Asefa and X. Zou, *Adv. Funct. Mater.*, 2016, **26**, 4839.

28 H. Jin, J. Wang, D. Su, Z. Wei, Z. Pang and Y. Wang, *J. Am. Chem. Soc.*, 2015, **137**, 2688-2694.

29 D. Zhou, L. He, W. Zhu, X. Hou, K. Wang, G. Du, C. Zheng, X. Sun and A. M. Asiri, *J. Mater. Chem. A*, 2016, **4**, 10114.

30 L. Jiao, Y. -X. Zhou and H. -L. Jiang, *Chem. Sci.*, 2016, **7**, 1690.